

## Fusaricidins from *Paenibacillus polymyxa* ZJU11 mediate the biological control of postharvest mango anthracnose

Cui Sun<sup>a</sup>, Yihan Wang<sup>a</sup>, Yihu Pi<sup>a,b</sup>, Jinping Cao<sup>a,b</sup>, Yue Wang<sup>a,b</sup>, Chaoyi Hu<sup>a</sup>, Chongde Sun<sup>a,b,\*</sup>

<sup>a</sup> Hainan Institute, Zhejiang University, Yazhou Bay Science and Technology City, Sanya 572025, China

<sup>b</sup> Laboratory of Fruit Quality Biology/The State Agriculture Ministry Laboratory of Horticultural Plant Growth, Development and Quality Improvement, Zijingang Campus, Zhejiang University, Hangzhou 310058, China

### ARTICLE INFO

#### Keywords:

Mango fruit  
*Paenibacillus polymyxa*  
 Anthracnose  
*Colletotrichum* species  
 Fusaricidin

### ABSTRACT

Mango fruits are highly susceptible to infection by *Colletotrichum* species, leading to the severe economic losses. In this study, an antagonist of *Paenibacillus polymyxa* ZJU11 with strong biocontrol activity was identified and its antifungal mechanisms were investigated. *P. polymyxa* ZJU11 effectively suppressed the growth of pathogens of mango fruit *in vitro* and *in vivo*. The whole genome sequencing and LC-MS/MS results revealed that the active component in *P. polymyxa* ZJU11 exerting antifungal activity was Fusaricidin A, B, C and D. The cell membrane integrity of pathogens was demonstrated to be damaged after Fusaricidin extract treatment by PI staining, SEM and TEM observation. Additionally, transcriptomic analysis indicated Fusaricidin extract upregulated the gene expression in cell cycle, MAPK signaling pathway, and autophagy in *C. asianum* HIN6, induced cell death. This study provides a promising and suitable biocontrol agent to protect the postharvest mango fruit from fungal infection.

### 1. Introduction

Mango (*Mangifera indica* Linn.) belonging to the family of *Anacardiaceae* and genus of *Mangifera*, is an important tropical and subtropical fruit and known as “king of tropical fruits” (Lin et al., 2023a,b; Yang et al., 2021). Mango fruits are deeply favored by consumers due to its unique flavor and rich nutrition, possessing unparalleled market value. However, mango is highly vulnerable to anthracnose disease caused by *Colletotrichum* species during storage and transportation, resulting in black brown spot on the surface of the fruit and seriously decreasing the fruit quality (Chutima and Tida, 2023; Lin et al., 2023a,b; Wu et al., 2022). The “Jinhuang” mango variety was widely planted in Southern China and severely affected by the dominant pathogenic fungi of *Colletotrichum siamense*, *Colletotrichum fructicola* and *Colletotrichum asianum*, causing enormous economic losses every year. *Colletotrichum* species had latent characteristics, lurking on the surface or inside of immature mango fruit without any visible symptoms. When the fruit matures, they quickly infected the fruit, leading to the rapid decay of the fruit and flesh tissue within three to seven days (Xie et al., 2025). Historically, the strategy for controlling postharvest anthracnose disease of

mango fruit mainly relied on the controlled atmosphere (Faisal et al., 2025), full cold chain (Chikez et al., 2021), or chemically synthesized fungicides (Xie et al., 2025), such as Iprodione and Benzimidazoles. Due to the high economic-cost and side effects of chemical fungicides, including environmental pollution and harm to human health, the emergence of fungicide-resistant *Colletotrichum* strains, and fungicide residues on fruit surfaces, the application of these methods is limited (Aguirre-Guitron et al., 2019; Wu et al., 2022; Zhou et al., 2022). Therefore, it is highly imperative to develop cost-effective, non-toxic, and environmentally friendly technologies to prevent mango fruit from being infected by *Colletotrichum siamense*, *Colletotrichum fructicola* and *Colletotrichum asianum*.

In recent years, the biological control to postharvest fungal diseases of mango fruit utilizing antagonistic microorganisms has been extensively explored, encompassing multiple mechanisms including nutrient and spatial competition, induced resistance, production of antifungal compounds, and parasitism, etc. (Chutima and Tida, 2023). Many antagonistic microorganisms have been isolated and identified from natural environments. For instance, the yeast strain of *Debaryomyces hansenii* 1R11CB and the bacterium strain of *Stenotrophomonas rhizophila*

\* Correspondence to: College of Agriculture and Biotechnology, Zhejiang University, China.

E-mail address: [adesun2006@zju.edu.cn](mailto:adesun2006@zju.edu.cn) (C. Sun).

KM02 were both isolated from marine and have demonstrated efficacy in suppressing postharvest anthracnose decay caused by *Colletotrichum gloeosporioides* in mango fruit (Montiel et al., 2017). Application of *Bacillus velezensis* UMAF6639 significantly reduced pathogenic decay in postharvest mango fruit resulting from *Neofusicoccum* spp. infection (Guirado-Manzano et al., 2024). *Talaromyces indica* DMKU-RP35 from plant leaves has been reported to exhibit high-efficacy suppression of postharvest mango anthracnose caused by *Colletotrichum gloeosporioides*, demonstrating control efficacy comparable to the fungicide benomyl (Konsue et al., 2020). *Wickerhamomyces anomalus* WA-2 and *Pichia kluuyveri* PK-3 exhibited substantial potential for controlling postharvest decay in mango fruit caused by *Neofusicoccum parvum* (Vecchio et al., 2025).

Among diverse biocontrol agents, *Paenibacillus polymyxa* has been classified as a Tier 1 exempt-from-safety-assessment strain by the Ministry of Agriculture owing to its superior biosafety profile and substantial biocontrol efficacy potential (Li and Chen, 2019). In plant disease management, substantial research demonstrates that *P. polymyxa* exhibited significant efficacy against fungal soil-borne diseases, consistently controlling field infections in crops including cucumber (Li and Chen, 2019), strawberry (Lee et al., 2024), tomato (Zhang et al., 2021). In postharvest disease management, *P. polymyxa* significantly reduces the incidence of soft rot in peach fruit and concurrently induces the expression of disease resistance-related genes (Wu et al., 2022). The U.S. Environmental Protection Agency (EPA) has registered it as a commercially applicable microbial species (Li and Jensen, 2008). However, most current studies on *P. polymyxa* remain at the stage of field control in plants, with few reports in the postharvest fruit domain. Furthermore, significant differences exist in the physiological characteristics among different *P. polymyxa* isolates. The types of antibacterial compounds produced in different microenvironments and the targets acting on pathogens also varied, which still require further investigation.

In this study, we evaluated the potential of *P. polymyxa* ZJU11 in suppressing mango anthracnose rot and explored the underlying mechanisms. Firstly, *P. polymyxa* ZJU11 was identified by 16S rRNA and determined its antagonistic activity *in vivo* and *in vitro*. Secondly, the Fusaricidin biosynthesis gene clusters involved in antagonistic activity of *P. polymyxa* ZJU11 were screened and validated through whole genome sequencing, and gene knockout. Thirdly, the antifungal effect of Fusaricidin extract was measured *in vivo* and *in vitro*, and the variant types of Fusaricidin were identified by GC-MS/MS. Fourthly, the impact of Fusaricidin extract on cell membrane integrity of *Colletotrichum* species was determined by propidium iodide staining, SEM and TEM observation. Fifthly, through transcriptomic analysis, the specific pathways and key genes related to antifungal effect in *C. aisanum* HNI6 were clarified. These findings provide a Tier 1 exempt-from-assessment strain to control postharvest anthracnose rot in mangoes as an alternative to chemical fungicides. Our data also offer a broader understanding of antagonistic mechanisms of *P. polymyxa* ZJU11 against the anthracnose pathogens.

## 2. Materials and methods

### 2.1. Strain and fruit

The pathogen of *Colletotrichum siamense* HNI2 (CCTCC No: M 20241875), *C. fructicola* HNI5 (CCTCC No: M 20241874) and *C. aisanum* HNI6 (CCTCC No: M 20241873) were originally isolated from decayed mango fruit. The antagonistic strain of *Paenibacillus polymyxa* ZJU11 (CCTCC No: M 20241847) was separated from the soil. At present, these strains are all preserved in ChinaCenter for Type Culture Collection (CCTCC).

“Jinhuang” mango fruit with 80 % mature was picked from an orchard in Jiyang District, Sanya City, China and transported to the laboratory within two hours. Fruits of uniform size, consistent maturity, without mechanical damage or pests and diseases were selected for

experimental research. Before use, the fruit was soaked in a 0.1 % NaClO for 2 min to remove surface dust and pathogens, rinsed with clean water to remove residual sodium hypochlorite, and finally disinfected with 75 % ethanol.

### 2.2. Phylogenetic construction of *Paenibacillus polymyxa* ZJU11

Total genomic DNA from *Paenibacillus polymyxa* ZJU11 was extracted with a CTAB method according to the kit instructions (SL2071, Coolaber). 16S rRNA from the genomic DNA was amplified with the high-fidelity DNA polymerase of KOD One PCR Master Mix Blue (Code No. KMM201S, TOYOBO) using the primer 27 F and 1492 R. The PCR amplification product was purified by agarose gel electrophoresis and gel recovery with a Gel recycling and purification kit (D2500-01, Omega BIO-TEK), and then connected to the plasmid of pEASY®-Blunt Zero. Recombinant plasmid was transformed into competent cells *Trans1-T1* and sequenced using primer pairs M13F and M13R. The sequencing result was uploaded to NCBI GenBank Database (GenBank number: PQ146574). The 16S rRNA sequences were aligned and trimmed using the PhyloSuite software, and then a phylogenetic tree was constructed using Mega-X. Finally, the ChiPlot platform (<https://www.chiplot.online/>) and Adobe Illustrator were used to beautify the evolutionary tree.

### 2.3. The inhibitory effect of ZJU11 on the anthracnose of postharvest mango fruit

A mechanical wound (1 mm wide × 3 mm deep) was made along the equatorial region of each mango fruit with a sterile inoculation needle. Each wound received 10 µL of a cell suspension of *Paenibacillus polymyxa* ZJU11 ( $5 \times 10^8$  cells mL<sup>-1</sup>), while control treatments were administered with an equal volume of sterile water. Twenty-four hours later, the wounds were individually inoculated with 10 µL of a spore suspension ( $1 \times 10^6$  spores mL<sup>-1</sup>) of one of the following fungal pathogens: *C. siamense* HNI2, *C. fructicola* HNI5 or *C. aisanum* HNI6. Following air-drying at ambient temperature, the fruits were incubated in darkness under controlled conditions at 25 °C and 85 % relative humidity. Disease progression was assessed daily from day three post-inoculation onward by measuring lesion diameters.

### 2.4. The antagonistic effect of ZJU11 on the pathogens of mango anthracnose *in vitro*

The antagonistic effects of ZJU11 against three anthracnose pathogens were evaluated using a dual-culture plate assay. The antagonist strain ZJU11 was streaked in parallel lines on both sides of a PDA plate and incubated at 28 °C for 24 h. Subsequently, an agar plug (0.7 cm in diameter) taken from the actively growing margin of a pathogenic fungus was placed at the center of the same plate. After incubation at 28 °C for 4 days, the inhibition index was determined based on the following formula: Inhibition index = (D3-D2)/D3 or D1/D3. D1 represents the colony radius of the control group pathogen, D2 represents the longitudinal radius of the pathogen in the treatment group, and D3 represents the distance from the center of the pathogen in the treatment group to *Paenibacillus polymyxa* ZJU11.

### 2.5. Whole genome sequencing of ZJU11 and prediction of anti-fungi metabolites

The antagonistic strain ZJU11 was grown in PDB medium at 28 °C with shaking at 200 rpm for 24 h. Then, the cells were harvested by centrifugation at 12,000 g for 2 mins. Genomic DNA was extracted from the ZJU11 pellets and submitted to Guangzhou Genedenovo Biotechnology Co., Ltd. for genome sequencing. Sequencing was carried out using both third-generation PacBio and second-generation Illumina technologies. Quality control of Illumina reads was performed with

Fastp, while Falcon was utilized for splicing and assembling third-generation sequencing reads. The assembled genome was polished using Pilon (version 1.23) by mapping short reads to the draft assembly under default parameters. The anti-SMASH online platform was utilized to predict the biosynthetic gene clusters responsible for the secondary metabolites.

## 2.6. Construction of mutant of ZJU11 related to the predicted biosynthesis gene cluster

To identify which predicted secondary metabolite synthesis gene clusters contribute to the inhibition of mango anthracnose, the core regions of five highly homologous gene clusters in the genome were selected for partial knockout via homologous recombination. The knockout cassette was designed to include an upstream homologous arm, a downstream homologous arm, and a chloramphenicol resistance gene fragment. The upstream and downstream homologous arms, each approximately 1000 bp in length, flank the 5' and 3' ends of the target deletion region, respectively. The chloramphenicol resistance gene was amplified from the plasmid pDG1661. These three fragments were assembled by fusion PCR and subsequently cloned into the vector PRN5101 using the pEASY®-Uni Seamless Cloning and Assembly Kit (CU101-01, Transgen, China). The constructed plasmid was transformed into Trans1-T1 competent cells. After verification, the recombinant plasmid was extracted and introduced into the antagonist strain *Paenibacillus polymyxa* ZJU11 by electroporation at 2000 V for 5 ms. Transformants were cultured at 39 °C with shaking at 200 rpm and subcultured every 24 h. Following several rounds of cultivation, double-crossover mutants were screened by PCR. All strains, plasmids, and primers used in this study are listed in [Supplementary Tables S1 and S2](#).

## 2.7. Antifungal activity of Fusaricidin extract on the pathogens of mango anthracnose *in vitro* and *in vivo*

The Fusaricidin extract was prepared referring the method from Lin et al. (2023) with some modifications. *P. polymyxa* ZJU11 was first cultured in PDB medium at 28 °C for 24 h as the seed culture. Then 20 mL of the seed culture was inoculated into 1 L of fresh PDB and fermented under identical conditions for 96 h. After fermentation, the strain was centrifuged at 8000 g for 10 min, and the supernatant was collected for subsequent extraction. To isolate Fusaricidin, *n*-butanol was mixed with the supernatant at a ratio of 1:4 (v/v) and stirring for 2 h. Then the mixture was settled for 12 h in a separatory funnel and the organic layer was recovered. This extraction process was repeated three times, and all organic phases were pooled. The combined *n*-butanol phase was concentrated using a rotary evaporator to obtain crude Fusaricidin extract, which was finally redissolved in methanol for further use.

The direct inhibitory effect of the Fusaricidin extract on three mango anthracnose pathogens was evaluated using the cup-plate assay. Briefly, spore suspensions of *C. siamense*, *C. fructicola*, and *C. asianum* with a concentration of  $1 \times 10^6$  spores mL<sup>-1</sup> were spread evenly onto PDA plates. After the surfaces were dried, sterile Oxford cups were placed at the center of each plate and lightly pressed. Then, 150 µL of the filter-sterilized (0.22 µm membrane) Fusaricidin extract solution was added into each cup. The plates were incubated in darkness for 3 days. The inhibition zones were measured after three days.

The inhibitory activity of Fusaricidin extract against mango anthracnose was assessed using a previously established method by Wang et al. (2020) with some modifications. Briefly, a sterile inoculation needle was used to create a uniform wound at the center of each surface-sterilized mango fruit. The Fusaricidin extract (5 mg·mL<sup>-1</sup>) was combined with the pathogenic spore suspension to achieve a final concentration of  $1 \times 10^6$  spores·mL<sup>-1</sup>. Then 10 µL of the mixture was inoculated into the wound, and the mixture of sterile water and the pathogenic spore suspension serving as the control. The fruits were

maintained in a climate-controlled incubator at 28 °C and 85 % relative humidity. Afterwards, observe the infection symptoms in the fruit wounds every day and record the lesion diameters.

## 2.8. Identification of fusaricidin compounds by LC-MS/MS

The types of Fusaricidins in the fermentation supernatant were detected using LC-MS/MS under positive mode. The measured parameters are as follows: spray voltage 3500 V, ion transfer tube temperature 320 °C, vaporizer temperature 300 °C, resolution 17,500.

## 2.9. Observation of cell membrane damage of the pathogens of mango anthracnose by Fusaricidin extract treatment

The membrane integrity of mango anthracnose pathogen spores was evaluated using a propidium iodide (PI) staining assay reported by Wang et al. (2020). Five mycelial plugs (7 mm diameter) obtained from the pathogen plate were added into 80 mL of PDB and incubated at 28 °C with shaking at 200 rpm for 5 days. The spore was collected by filtering through a sterile cell filter and washed twice with sterile water to remove medium residues. The spores were then treated with Fusaricidin extract (5 mg·mL<sup>-1</sup>) for 2 h, collected by centrifugation at 8000 g, and washed again. For PI staining, 10 µL of PI solution (20 mg·mL<sup>-1</sup>) was mixed to 1 mL of the spore suspension and placed in darkness for 30 min. After two washes with PBS (pH 7.0), the stained spores were visualized using a confocal laser scanning microscope (Stellaris 5, Leica, Germany).

To assess the impact of Fusaricidin extract on the morphological and ultrastructural characteristics of anthracnose spores, both scanning and transmission electron microscopy (SEM and TEM) were applied. For SEM sample preparation, fungal spores were immobilized by overnight fixation at 4 °C in 2.5 % glutaraldehyde, followed by washing three times with phosphate buffer (0.1 mol L<sup>-1</sup>, pH 7.0). Subsequent fixation was performed using 1 % osmium tetroxide, after which the samples were again rinsed three times. Dehydration was then carried out through a graded ethanol series (30 %, 50 %, 70 %, 80 %, 90 %, 95 %, and 100 %). The spores were finally resuspended in a minimal volume of absolute ethanol and subjected to critical-point drying. Prior to imaging, the samples were sputter-coated with a conductive layer and examined under a scanning electron microscope.

For TEM sample preparation, the procedures for fixation and rinsing of spores followed the same protocol as previously described for SEM. Spore dehydration was carried out through a graded ethanol series (30 %, 50 %, 70 %, 80 %, 90 %, 95 %, and 100 %), followed by further dehydration in an acetone gradient (90 %, 95 %, and 100 %). Subsequently, the samples were infiltrated with mixtures of Spurr's resin and acetone at volume ratios of 1:1 and 1:3. Finally, the spores were embedded with pure embedding agent. The embedded samples were sliced in an ultramicrotome, stained with lead citrate solution and uranyl acetate solution for 5 min each, and observed under transmission electron microscopy.

## 2.10. Transcriptomic (RNA-seq) analysis

To further investigate the inhibitory mechanisms of ZJU11 on mango anthracnose, *C. asianum* was selected as a typical representative and treated with Fusaricidin extract for RNA-seq. Spores were collected from PDB medium cultured for 5 days and treated with 5 mg mL<sup>-1</sup> of Fusaricidin extract for 10 min. The sterile water was used as the control. Total RNA was extracted with Omega Plant RNA kit (R6827, Omega Bio-Tek, USA) and the purity was detected by spectrophotometer (NanoDrop eight, Thermo Scientific, China). The RNA integrity, purification, cDNA synthesis, library construction and sequencing were conducted by Guangzhou Genedenovo Biotechnology Co., Ltd. The reference genome was *Colletotrichum asianum* TYC-2 (version: GCA\_OU5514765.1). RSEM (version: 1.2.19) and DESeq (version: 1.20.0) software was used for gene quantitative analysis and differential analysis, respectively. Furthermore, biological functional enrichment analysis of differentially

expressed genes (DEGs) was performed by GO and KEGG database.

### 2.11. Statistical analysis

All data statistic in this assay were performed based on Student's *t*-test and graphed by GraphPad Prism (version 8.2.1). Data were expressed as mean  $\pm$  SEM. Difference was considered significant at the level of  $p < 0.05$ .

## 3. Results

### 3.1. Identification of *P. polymyxa* ZJU11

The 16S rRNA of ZJU11 was amplified, and a target fragment with a length of 1515 bp was obtained. Then the sequence was submitted to the NCBI database and obtained the GenBank number (PQ146574). Subsequently, the sequencing results were subjected to BLAST alignment on NCBI database, and 29 strains with high similarity and detailed information were selected as references, and Mafft was then used for multiple

alignment to construct a phylogenetic tree. The phylogenetic tree shows that ZJU11 was clustered on the same branch as *Paenibacillus polymyxa* MEZ6 and *Paenibacillus polymyxa* ACCC03434, suggesting a close genetic relationship (Fig. 1). Meanwhile, morphological identification results showed that the colonies of ZJU11 were white, round, smooth on the surface, and had irregular edges (Fig. 2A). SEM results showed that the cells of strain ZJU11 were short rod-shaped with wrinkled surfaces. The transmission electron microscopy results are consistent with scanning electron microscopy, and the cell wall edges of strain ZJU11 have fine hair-like structures attached to them, which may be related to increased cell surface area and good colonization ability. Based on the comprehensive molecular biology identification results and morphological characteristics, ZJU11 was identified as *Paenibacillus polymyxa*.

### 3.2. ZJU11 inhibit the growth of the dominant pathogens of mango anthracnose *in vivo* and *in vitro*

To investigate the antagonistic ability of the *P. polymyxa* ZJU11, three dominant strains of pathogenic fungi of mango anthracnose,

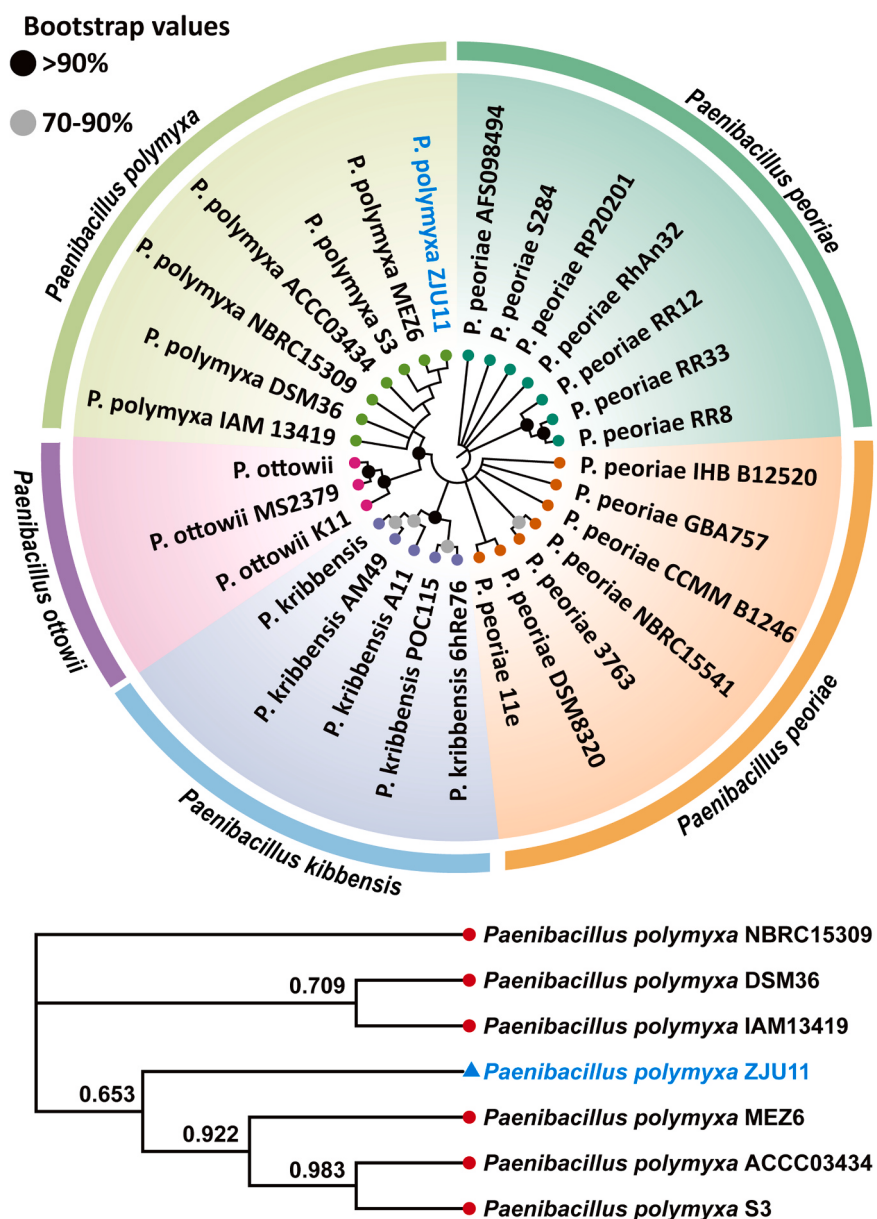


**Fig. 1.** Phylogenetic tree of *Paenibacillus polymyxa* ZJU11 based on 16S rRNA gene. ▲ was representative strains isolated in this study.

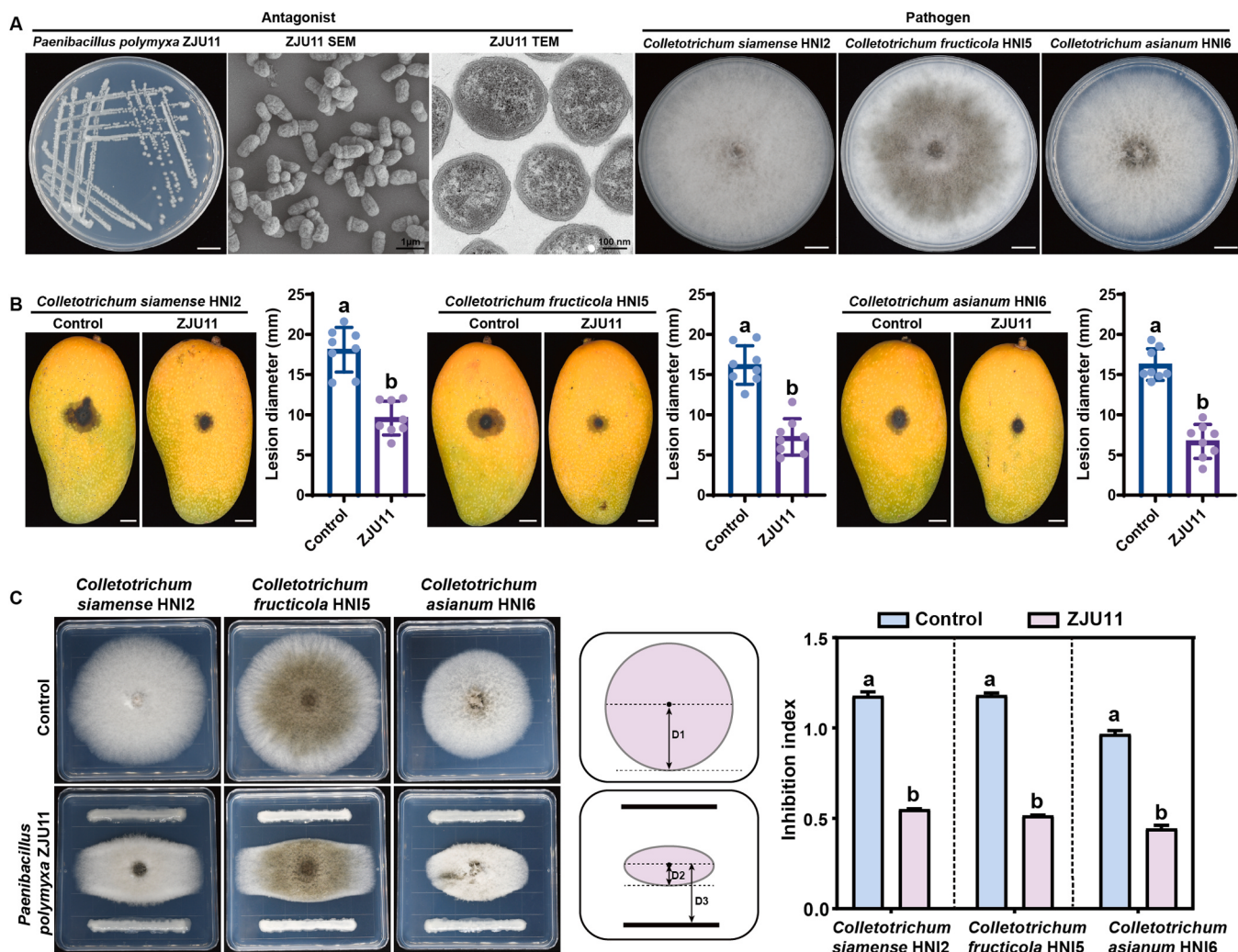


**Fig. 2.** The antagonistic effect of *Paenibacillus polymyxa* ZJU11 against three dominant anthracnose pathogens in mango fruit and PDA plate. (A) The colony morphology of *P. polymyxa* ZJU11 and pathogens of *Colletotrichum siamense* HNI2, *Colletotrichum fructicola* HNI5 and *Colletotrichum asianum* HNI6. (B) Biocontrol efficacy of *P. polymyxa* ZJU11 on anthracnose disease in mango fruit. (C) Inhibition effect of *P. polymyxa* ZJU11 against *C. siamense* HNI2, *C. fructicola* HNI5 and *C. asianum* HNI6. Error bar represents the standard deviation of three biological replicates. The different letters in the column indicate significant differences ( $p < 0.05$ ) as determined by Student's *t*-test.

namely *C. siamense* HNI2, *C. fructicola* HNI5 and *C. asianum* HNI6, were separated from the decayed mango fruit in this study and the colony morphology was present in Fig. 2A. Biological control test results *in vivo* shown that *P. polymyxa* ZJU11 exhibited a broad-spectrum antifungal ability against these three pathogenic fungi and significantly decreased the lesion diameter of postharvest mango fruit caused by anthracnose disease after inoculated with spores of *C. siamense* HNI2, *C. fructicola* HNI5 and *C. asianum* HNI6 for 4 days, respectively (Fig. 2B). Compared with the control, the lesion diameter of mango fruit was decreased by 46.99 % for inoculating with *C. siamense* HNI2, 55.28 % for inoculating with *C. fructicola* HNI5, 58.86 % for inoculating with *C. asianum* HNI6. Moreover, the results from the plate confrontation test showed that ZJU11 strongly inhibited the expansion of the indicator pathogen hyphae, and there was an antifungal band between ZJU11 and the indicator pathogen, with the inhibition index more than 50 % for *C. siamense* HNI2 and *C. fructicola* HNI5 (Fig. 2C), suggesting ZJU11 possess excellent antagonistic ability.

### 3.3. Fusaricidin biosynthesis gene cluster was involved in antagonistic activity of ZJU11

In order to further reveal the antagonistic mechanisms of ZJU11,

whole genome sequencing was performed to uncover more antagonistic related genes. The whole genome of ZJU11 contained one chromosome with a size of 5753276 bp and GC content of 45.43 %. The sequence has been submitted to the NCBI database and the accession number was CP171416. The whole genome sequence predicted 4782 protein-coding genes, with a total length of 4903062 bp, a maximum length of 42396 bp, a minimum length of 48 bp, and a GC content of 46.60 %. There are 156 non-coding RNAs to be found, including 110 tRNAs, 42 rRNA, and 4 sRNAs. In the COG (Cluster of Orthologous Groups of proteins) function classification, the highest term involved in carbohydrate transport and metabolism (574 genes), followed by transcription (510 genes), general function prediction only (455 genes), signal transduction mechanisms (385 genes), amino acid transport and metabolism (370 genes) (Fig. 3A). In addition, there are 113 genes involved in the secondary metabolite biosynthesis, transport and catabolism in the genome, indicating that the metabolites produced by ZJU11 may contain antibacterial substances. It is worth noting that there are still 205 genes whose functions are unknown and require further investigation.

The metabolism gene clusters of ZJU11 were predicted using antiSMASH online platform, and 17 secondary metabolite synthesis gene clusters were found, of which 5 had a similarity of 100 % with gene

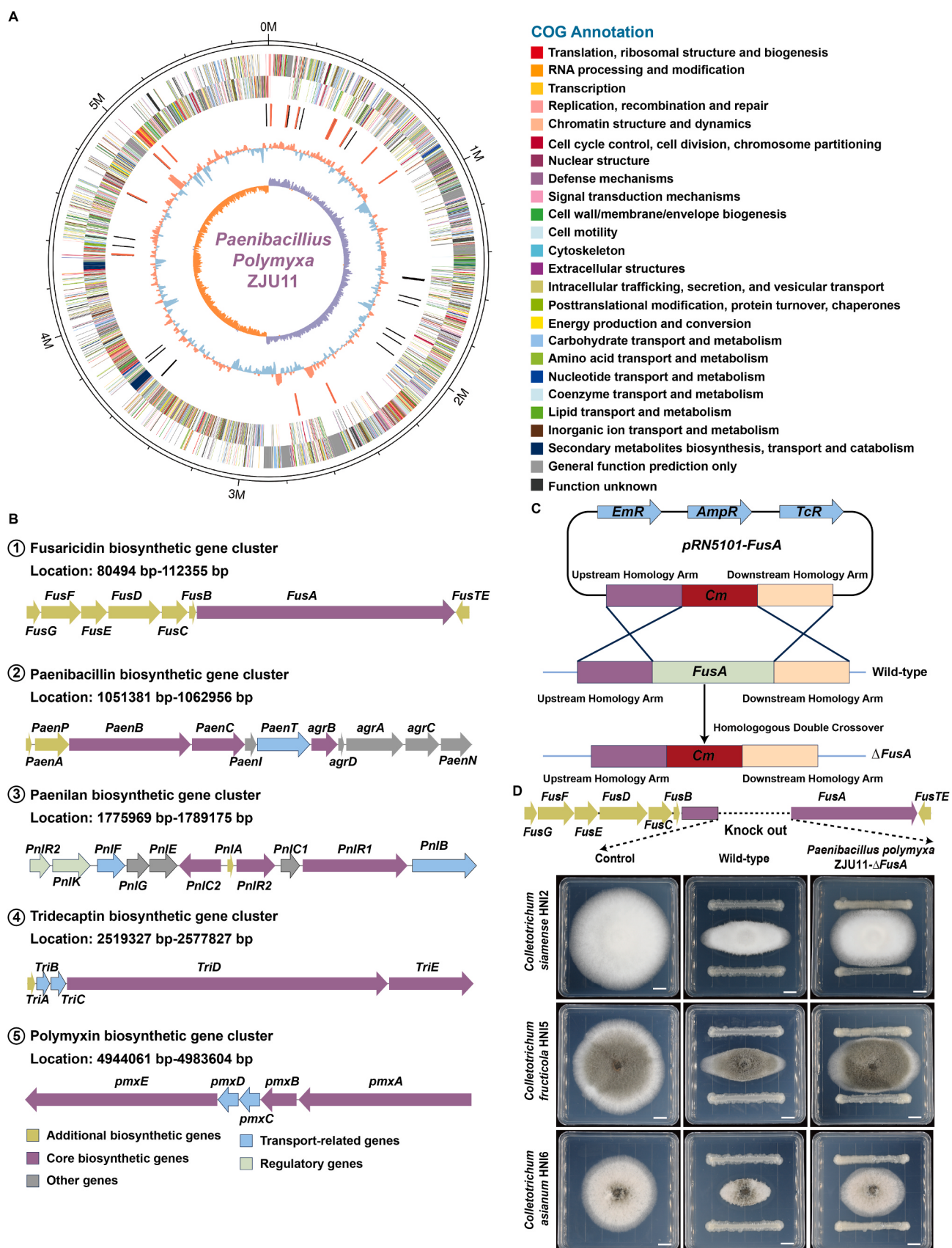


**Fig. 3.** Prediction of the biosynthetic gene cluster for secondary metabolite in *Paenibacillus polymyxa* ZJU11 and functional verification of its antagonistic efficacy. (A) The circular genome plot of *Paenibacillus polymyxa* ZJU11. (B) Five biosynthetic gene clusters predicted by Anti-SMASH in *P. polymyxa* ZJU11 genome. (C) Schematic diagram of the knockout strategy for *FusA*. (D) Validation of antagonistic activity of *FusA* mutant against *Colletotrichum siamense* HNI2, *Colletotrichum fructicola* HNI5 and *Colletotrichum asiaticum* HNI6 in vitro.

clusters of known antibacterial substances. Specifically, including Fusaricidin biosynthetic gene cluster, Paenibacillin biosynthetic gene cluster, Paenilan biosynthetic gene cluster, Tridecaptin biosynthetic gene cluster and Polymyxin biosynthetic gene cluster (Fig. 3B). The high similarity of these gene clusters suggests that *P. polymyxa* ZJU11 may produce corresponding antibiotics, including Fusaricidin, Paenibacillin, Paenilan, Tridecaptin and Polymyxin. Then, the core genes in these gene clusters were knocked out using homologous recombination technology to verify whether these gene clusters are involved in the antagonistic activity of ZJU11. The knockout strategy was shown in Fig. 3C. The knockout target gene sequence, upstream homologous arm sequence and downstream homologous arm sequence were amplified by PCR and verified by agarose gel electrophoresis. The related results were shown in Fig. S1 and S2. The results from gene cluster function showed that the *P. polymyxa*-ΔFusA mutant reduced its antagonistic activity against *C. siamense* HNI2, *C. fructicola* HNI5 and *C. asianum* HNI6, while other mutants, such as *P. polymyxa*-ΔPaenC, *P. polymyxa*-ΔPnlR1, *P. polymyxa*-ΔTriD and *P. polymyxa*-ΔPmxA, showed similar antagonistic activity to the wild-type strain *P. polymyxa* ZJU11 (Fig. 3D and Fig. S3). These results indicated that the Fusaricidin biosynthetic gene cluster was involved in the inhibitory effect of ZJU11 on mango anthracnose.

#### 3.4. The inhibition efficacy of fusaricidin extract on the anthracnose disease of mango fruit and the identification of the types of fusaricidin by LC-MS/MS

The secondary metabolites produced by ZJU11, especially Fusaricidin, may exert inhibitory effects on three dominant pathogens mentioned above. Therefore, the Fusaricidin extract was prepared using the organic solvent *n*-butanol. Compared with the control, Fusaricidin extract displayed significant antifungal activities on *C. siamense* HNI2, *C. fructicola* HNI5 and *C. asianum* HNI6, and the obvious antifungal zones around the dishes were appeared in PDA plates (Fig. 4A), indicating the indirect antifungal effect by Fusaricidin extract. Furthermore, after inoculating the mixture of Fusaricidin extract and pathogens into the wound of mango fruit for 4 days, it was found that there were no obvious decayed symptoms, while the control group showed larger lesion diameters with 14.09 mm for inoculating with *C. siamense* HNI2, 15.75 mm for inoculating with *C. fructicola* HNI5 and 13.81 mm for inoculating with *C. asianum* HNI6 (Fig. 4B). To identify the types of Fusaricidin compounds in the Fusaricidin extract, the Fusaricidin extract was subjected to GC-MS/MS. It was found that four ion peaks with 883.6 Da at 9.533 min, 897.6 Da at 10.024 min, 947.6 Da at 9.027 min and 961.6 Da at 9.030 min were detected in the mass spectrogram, which might be that ZJU11 produced four different types of Fusaricidins (Fig. 4C). These four spectra were retrieved from the mass spectrometry database and identified as Fusaricidin A, B, C and D. For Fusaricidin A, ion of *m/z* 883.6 Da was the precursor ions, ion of *m/z* 628.3411 Da represented molecular chain of peptide moiety 1 (Pemo1) and *m/z* 256.2482 Da represented 15-guanidine-3-hydroxypentadecanoic acid (GHPD). Fusaricidin B, ion of *m/z* 897.6 Da was the precursor ions, ion of *m/z* 642.3476 Da represented molecular chain of Pemo2 and *m/z* 256.2406 Da represented GHPD. Fusaricidin C, ion of *m/z* 947.6 Da was the precursor ions, ion of *m/z* 692.3241 Da represented molecular chain of Pemo3 and *m/z* 256.2409 Da represented GHPD. Fusaricidin D, ion of *m/z* 961.6 Da was the precursor ions, ion of *m/z* 706.3408 Da represented molecular chain of Pemo4 and *m/z* 256.2388 Da represented GHPD.

#### 3.5. Fusaricidin extract destroyed the cell membrane integrity of pathogens of mango anthracnose

Propidium iodide (PI) is a membrane-impermeant dye that selectively enters cells with compromised membranes, where it intercalates with nucleic acids and produces red fluorescence. Based on this property, PI staining was applied to assess the disruptive effects of

Fusaricidin extract on the membrane integrity of anthracnose spores. As illustrated in Fig. 5A, no obvious or only weak fluorescence signals were detected in the control group, regardless of *C. siamense* HNI2, *C. fructicola* HNI5 and *C. asianum* HNI6, indicating structurally intact membranes. In contrast, treatment with Fusaricidin extract resulted in intense PI-derived fluorescence across all three pathogens, demonstrating severe disruption of membrane integrity.

The morphology and ultrastructure of the three pathogen spores were significantly changed after treatment with Fusaricidin extract. The SEM results showed that spores in the control group were plump and regular oval shaped, while the spores in the treatment group had ruptured on the surface and their morphology was disrupted and the three pathogenic spores all exhibited similar features (Fig. 5B). TEM results showed that untreated spores have normal cell morphology, intact and smooth cell walls, and intact cell membranes. However, it can be observed that the cell membranes of spores were ruptured, the cytoplasmic wall separated, and the organelles become blurred (Fig. 5B).

#### 3.6. RNA-seq analysis

Based on the strong inhibitory effect of Fusaricidin extract against the three pathogens of mango anthracnose disease mentioned above, *C. asianum* HNI6 were selected as a representative to study the anti-fungal mechanism by RNA-seq analysis. There were 2286 upregulated genes and 643 downregulated genes to be identified in the transcriptome file of *C. asianum* HNI6 after Fusaricidin extract treatment (FDR<0.05) (Fig. 6A). These DEGs were classified and annotated by GO and KEGG database. In the GO classification, the term with the highest gene enrichment was biological regulation (GO: 0065007, 1080 DEGs), followed by nucleobase-containing compound metabolic process (GO:0006139, 1111 DEGs), regulation of biological process (GO:0050789, 986 DEGs), and cellular component organization or biogenesis (GO:0071840, 964 DEGs) (Fig. 6B). Within the KEGG pathway, cell cycle (Pathway ID: ko04111, 48 DEGs), ribosome biogenesis in eukaryotes (Pathway ID: ko03008, 33 DEGs), and meiosis-yeast (Pathway ID: ko04113, 32 DEGs) (Fig. 6C). Several enzymes involved in cell growth and death, including cell cycle checkpoint protein, mediator of replication checkpoint protein 1, serine/threonine-protein kinase CHEK2 and regulatory factor X 1/2/2 were found to be activated in response to Fusaricidin extract treatment (Fig. 6D). Four genes enriched this pathway were shown by heatmap, namely RB213\_008268 (*Dun1*), RB213\_010863(*Rad24*), RB213\_014998(*Rfx1*) and RB213\_008045(*Mrc1*). Additionally, the enriched KEGG pathway also included MAPK signaling pathway and autophagy-other, which contributed to the cell wall stress, hi osmolarity and cell death (Fig. 6E). RB213\_003058, RB213\_004163, RB213\_002624, and RB213\_005132, etc. were associated with the MAPK signaling pathway. RB213\_000197, RB213\_002278, RB213\_006487 and RB213\_007580 etc. were related to the cell autophagy.

#### 4. Discussion

*P. polymyxa* as a safe and environmental-friendly biocontrol agent has been reported to inhibit plant pathogenic fungi in agricultural production due to its strong antagonistic activity. *P. polymyxa* has showed strong and broad-spectrum antagonistic activity *in vitro* against *Fusarium asiaticum*, *Fusarium moniliforme*, *Verticillium albo-atrum*, *Fusarium graminearum*, *Monilia persoon*, *Alternaria mali*, *Botrytis cinerea*, and *Aspergillus niger* (Li and Chen, 2019). Different strains of *P. polymyxa*, such as *P. polymyxa* AF01 (Lin et al., 2023), *P. polymyxa* PJH16 (Yang et al., 2024) and *P. polymyxa* YJ1-5 (Zhang et al., 2021), have been demonstrated the good biocontrol potential in controlling pitaya canker caused by *Neoscytalidium dimidiatum*, cucumber fusarium wilt caused by *Fusarium oxysporum* f. sp. *cucumerinum*, tomato gray mold caused by *Botrytis cinerea*, respectively. In this study, we also isolated an antagonistic strain

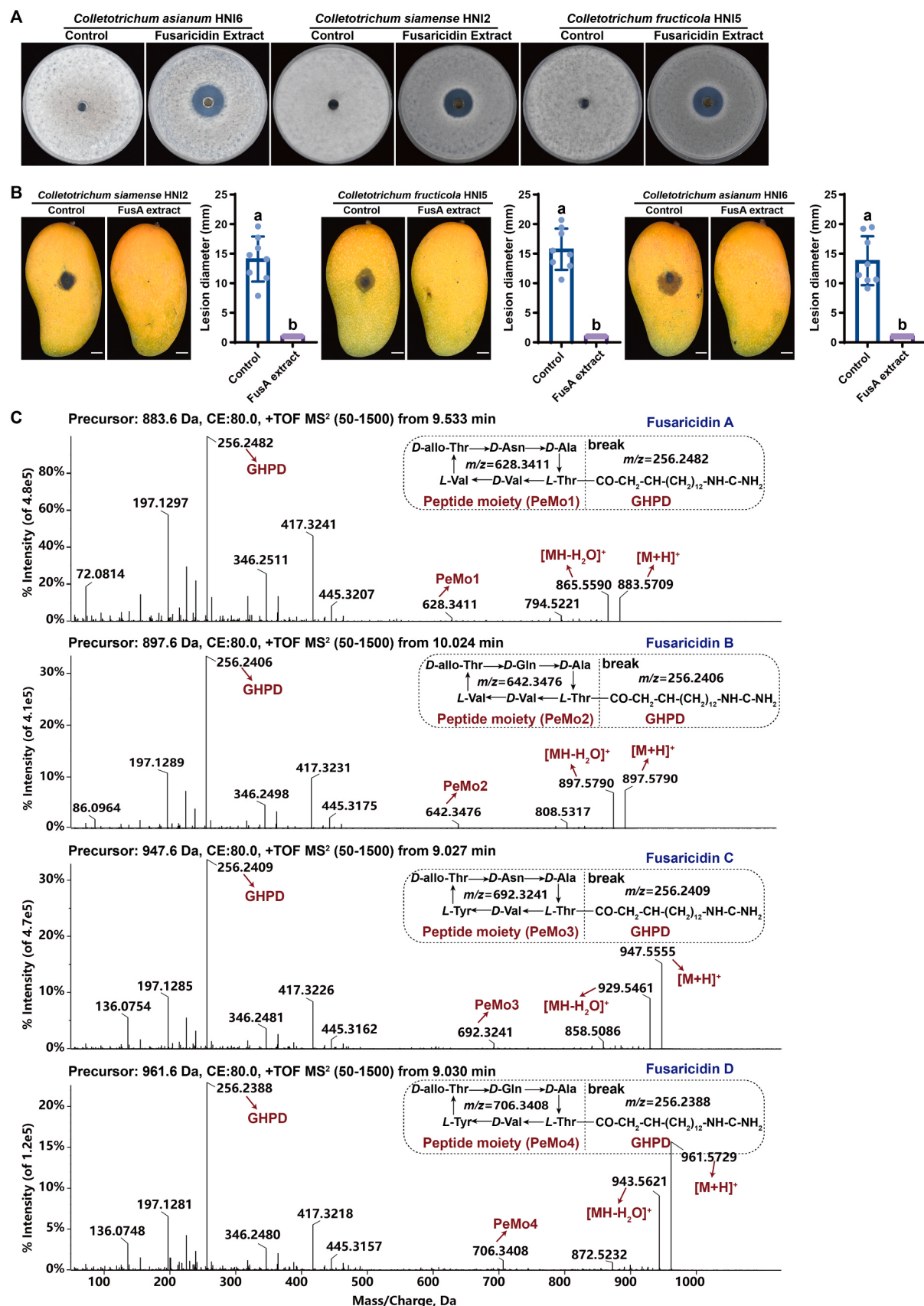


**Fig. 4.** Analysis of antifungal activity and identification of Fusaricidin types in a crude extract. (A) Antifungal ability of Fusaricidin extract against *Colletotrichum siamense* HNI2, *Colletotrichum fructicola* HNI5 and *Colletotrichum asiannum* HNI6 in PDA plate. (B) Control efficacy of Fusaricidin extract on mango anthracnose disease caused by three pathogens. (C) Identification of Fusaricidin types by LC-MS/MS. FusA represent Fusaricidin. The different letters in the column indicate significant differences ( $p < 0.05$ ) as determined by Student's t-test.

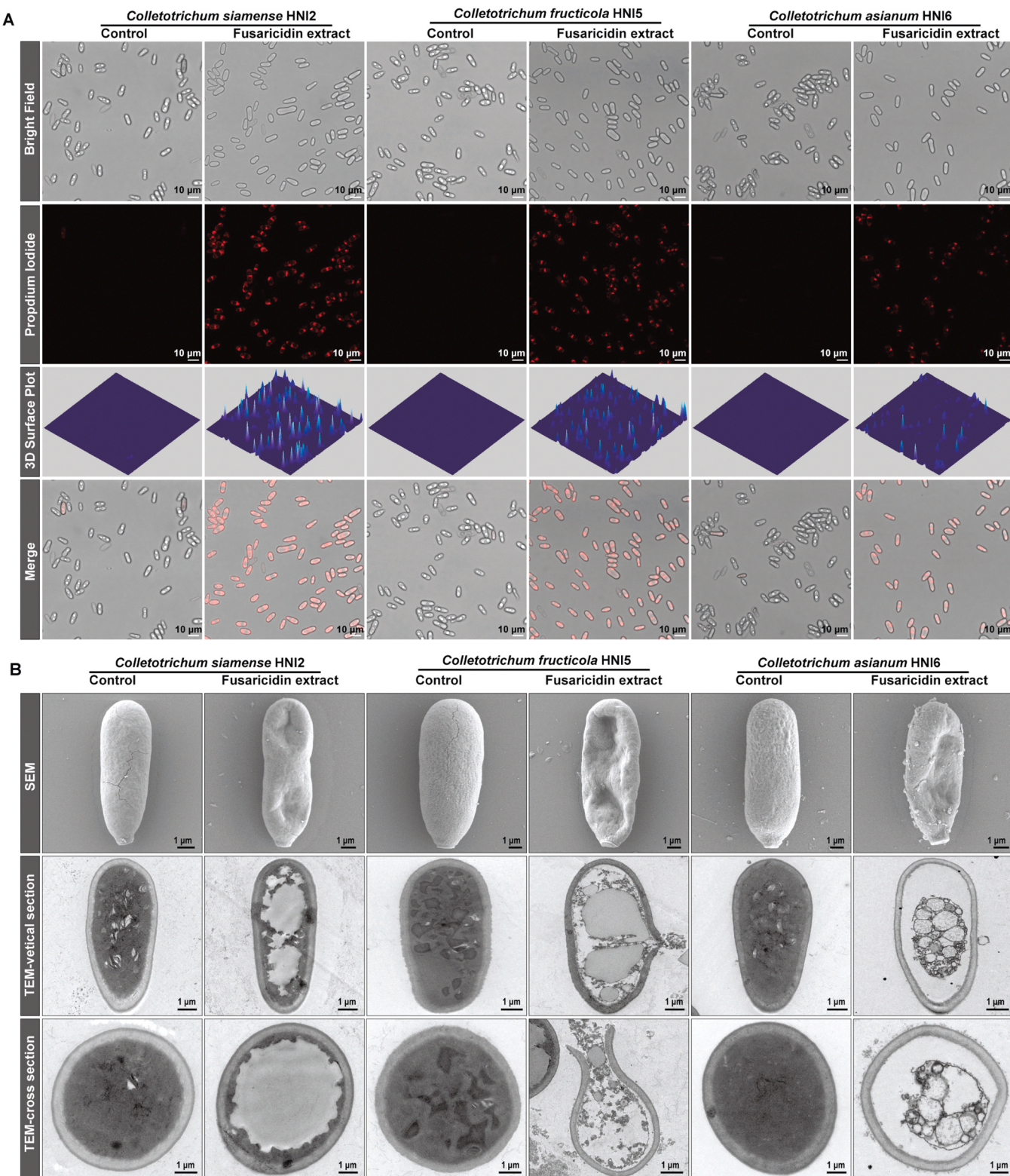


**Fig. 5.** Observation on the damage effect of Fusaricidin extract on anthracnose spores. (A) Microscopic observation of anthracnose spores treated with Fusaricidin extract after staining with propidium iodide (PI). (B) Morphological observation of anthracnose spores treated with Fusaricidin extract via scanning and transmission microscopy.

ZJU11 from Sanya, Hainan Province, China, and identified as *P. polymyxa* based on 16S rRNA and its morphological characteristics due to the highly similarity of these features with previous report by Lin et al. (2023). Furthermore, *P. polymyxa* ZJU11 displayed a broad-spectrum antifungal activity against three dominant pathogens of

*C. siamense* HNI2, *C. fructicola* HNI5 and *C. asianum* HNI6 *in vitro* and in mango fruit wounds. The results were similar with a previous study reported by Wu et al. (2020) that *P. polymyxa* CF05 could effectively suppress the postharvest mango rot caused by *Rhizopus stolonifer* and the mechanism of action might be related to the volatile organic compounds

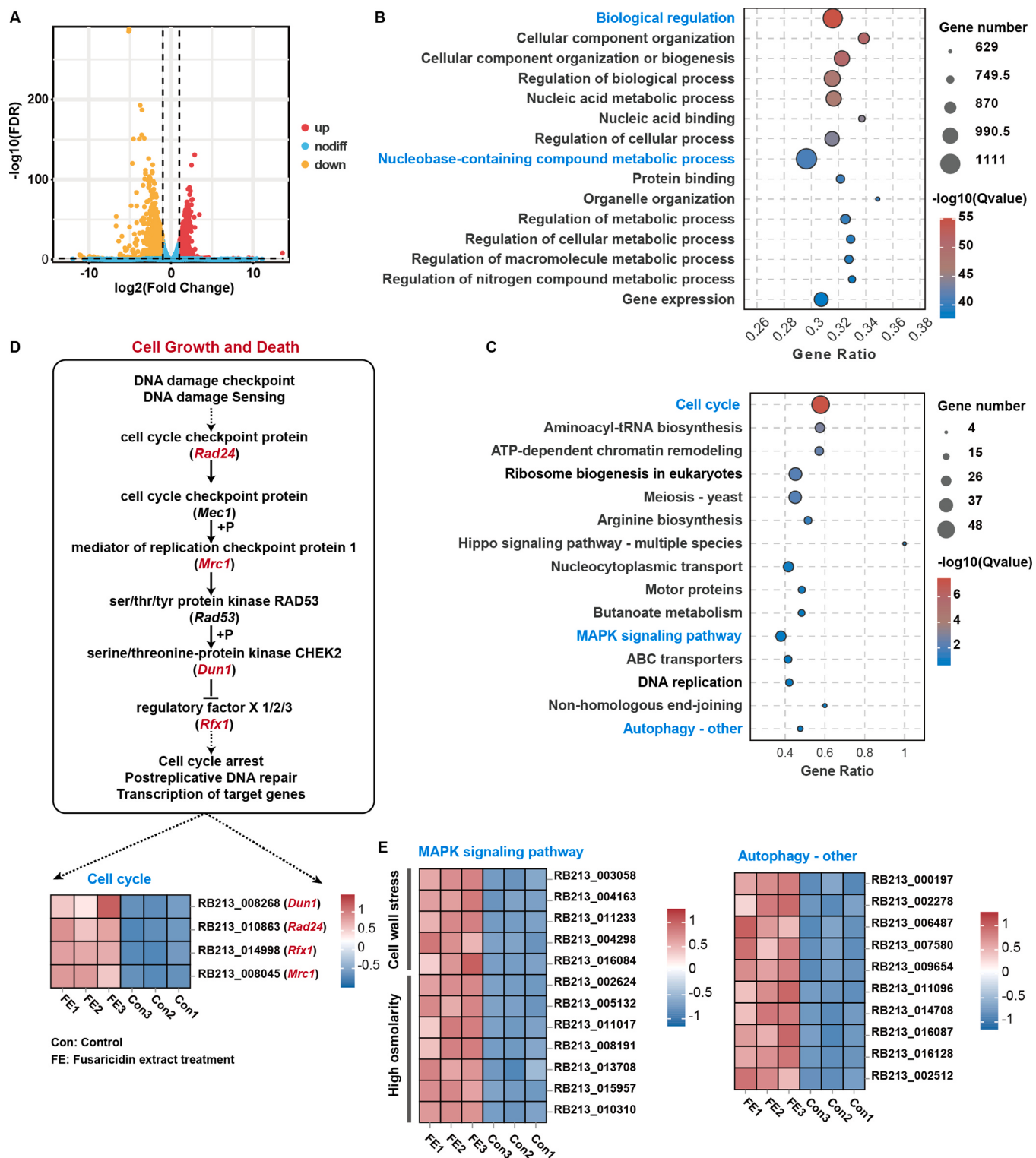


**Fig. 6.** Transcriptomic analysis of *Colletotrichum asianum* HNI6 in response to Fusaricidin extract, including volcano plot (A), Gene Ontology (GO) enrichment analysis (B), KEGG enrichment analysis (C), and heatmaps analysis of cell growth and death (D), and MAPK signaling pathway and autophagy-other (E).

it produced. Therefore, these results obtained in this study demonstrated the antagonistic strain of *P. polymyxa* ZJU11 as a biological control agent is a promising alternative strategy to control postharvest mango anthracnose rot.

Previous studies indicated that antagonistic microorganisms could effectively suppress the growth of plant pathogen, largely due to their ability to synthesize bioactive secondary metabolites, especially for the

antifungal proteins (cellulase, chitinase,  $\beta$ -1,3/1,6-glucanase) and lipopeptides (Polymyxins, Surfactins, Fusaricidins, Fengycins, Tridecaptins, etc) (Li and Chen, 2019). These compounds could interfere with lipid metabolism, membrane transport, energy metabolism, etc. of the pathogenic fungi (Zuo et al., 2017). Yang et al. (2024) identified 19 gene cluster related to the biosynthesis of secondary metabolites by genome sequencing and anti-SMASH prediction from *P. polymyxa* PJH16,

including 9 gene clusters encoding NRPS (non-ribosomal peptide synthase), among which Fusaricidin B, Paenibacillin, Tridecaptin and Polymyxin had a similarity of 100 % with known antibiotics. Antifungal compounds of Fusaricidins (*m/z* of 883, 897, 901, 915, 947, 965, and 979 Da) and L1-F antibiotic (*m/z* of 929 Da) were also detected from *P. polymyxa* YJ1-5 by MALDI-TOF MS and proven to disrupt the cell membranes integrity of *B. cinerea* (Zhang et al., 2021). In the present study, we sequenced the genome of *P. polymyxa* ZJU11 and predicted 17 secondary metabolite gene clusters, including 5 compounds with a 100 % match to known antibiotics. These antibiotic synthesis gene clusters encoded Fusaricidin, Paenibacillin, Paenilan, Tridecaptin and Polymyxin and it was confirmed through gene knockout assay that only Fusaricidin biosynthesis gene cluster was involved in the antagonistic activity of *P. polymyxa* ZJU11 against *Colletotrichum* species. The results were consistent with the report by Li et al. (2019) that among several antimicrobial biosynthesis mutants constructed in *P. polymyxa* WLY78, only the Fusaricidin-deficient mutant (fusA<sup>-</sup>) lost its antagonistic activity, while all other mutants retained activity comparable to the wild-type strain. These findings suggest that Fusaricidin biosynthetic gene cluster mediated the inhibitory effect of *P. polymyxa* ZJU11 against the mango anthracnose pathogens, including *C. siamense* HNI2, *C. fructicola* HNI5 and *C. asianum* HNI6.

Although *P. polymyxa* can produce antibiotic, such as Polymyxin, Tridecaptin, Fusaricidin and Polymyxin, the antagonistic compounds related to biocontrol mainly depend on the Fusaricidin and Polymyxin (Li and Chen, 2019; Muelner et al., 2021; Yang et al., 2018). This statement was partially consistent with the results in this study mentioned above. Fusaricidin is a non-cationic cyclic hexapeptide compound containing a complex of over 20 variants (Li and Jensen, 2008). Structurally, they all contain 15-guanidine-3-hydroxypentadecanoic acid (GHPD), which binds to a threonine (Thr) ring consisting of six amino acids (Li and Chen, 2019). GHPD is strictly conserved, but different variants are formed due to differences in amino acids and their sequences (Li and Jensen, 2008; Vater et al., 2015). According to the different *m/z* values in the mass spectrometry, Vater et al. (2015) classified the peaks within the range of *m/z* 860–925 into series 1, including Fusaricidin A (LI-F04a), Fusaricidin B (LI-F04b), LIF05a, LI-F06a, LI-F05b, LI-F06b, LI-F08b, and one unknown compound (*m/z* 869.8). The peaks within the range of *m/z* 947–975 were classified into series 2, including Fusaricidin C (LI-F03a), LIF07b, Fusaricidin D (LI-F03b), and one unknown compound (*m/z* 975.8). The peaks within the range of *m/z* 931–959 were classified into series 3, including LI-F07a, LI-F07b, and one unknown compound (*m/z* 959.8). *P. polymyxa* isolated from different source could produce different types of Fusaricidins, and exhibited different antifungal ability. *P. polymyxa* Y-1, obtained from the stem of *Dendrobium nobile*, was found to produce six types of Fusaricidins (Fusaricidin A, B, C, D, L1-F05 and L1-F06), and exhibited strong antifungal activity against fungi of the genus on *Pestalotiopsis* (Yang et al., 2018). Fusaricidin (A and B mixtures) and four analogs were also detected from *P. polymyxa* E681 (Ko et al., 2019), while Fusaricidin A and its derivatives were found in *P. polymyxa* DSM32871 and M1 (Muelner et al., 2021). Although these *P. polymyxa* can produce Fusaricidin A and its derivatives, the intensity of the mass spectrometry peaks of each variant varies significantly among strains. In our study, we found that the *n*-butanol extract from the fermentation broth of *P. polymyxa* ZJU11 showed intensive antifungal activity on anthracnose pathogens of mango fruit, and four variants of Fusaricidin A, B, C and D were identified by GC-MS/MS. Based on current data and previous studies, it is confirmed that the inhibitory effect of *P. polymyxa* ZJU11 on mango anthracnose is mainly attributed to Fusaricidins.

The membrane systems of fungal cells contain a diverse array of lipid species, such as glycerophospholipids, sphingolipids, and sterols. These lipids play essential roles in regulating cellular homeostasis, facilitating material exchange, supporting energy transformation, and enabling signal recognition. (Ji et al., 2020; Sant et al., 2016; Wang et al., 2020). Due to its amphiphilic properties, the cell membrane has become one of

the targets of antibacterial compounds. Zou et al. (2022) believed that the hydrophobicity of antibacterial agents gives them a high affinity for cell membranes, thereby increasing their permeability. This statement has been confirmed in the research of many antifungal compounds. Paeonol (Qian et al., 2021), citral (Zeng et al., 2023), berberine (Xie et al., 2025) and phenazine-1-carboxylic acid (Huang et al., 2025) were hydrophobic compounds that can damage the integrity of fungal cell membranes, causing leakage of fungal cell contents, increased conductivity, and ultimately leading to cell death. Consistent with previous research findings, the present study found that Fusaricidin extract, as a hydrophobic compound, disrupted the cell membrane structure of pathogens of *C. siamense* HNI2, *C. fructicola* HNI5 and *C. asianum* HNI6, and increased the permeability of the cell membrane. SEM and TEM confirmed the membrane damage by Fusaricidin extract, which led to alter in morphology and leakage of cell contents. According to reports, the target site of this hydrophobic antifungal agent may be ergosterol, which has the highest content in the cell membrane (Sant et al., 2016). As for whether the target of Fusaricidin extract is binding to ergosterol, further research is needed.

The antifungal mechanism involved multiple metabolic and signal transduction pathways, including cell cycle, oxidative stress, citrate cycle pathway (TCA cycle), MAPK signaling pathway, and DNA repair, and cell autophagy, etc. (Ma et al., 2020; Xie et al., 2025). Previous study found that cell cycle of *Penicillium expansum* was interfered by chitosan in cell cycle experiments, causing damage to DNA in the G1 phase (Gong et al., 2024). The serine/threonine phosphorylation belonging to MAPK signal transport was reduced in *Colletotrichum gloeosporioides* by antifungal treatment (Xie et al., 2025). In addition, autophagy also plays a critical role in multiple fundamental biological processes in filamentous fungi, including development (both asexual and sexual), pathogenicity, stress adaptation to nutrient limitation, and the regulation of programmed cell death. (Ma et al., 2020; Ren et al., 2018; Zhang et al., 2022). A study by Ma et al. (2020) demonstrated that honokiol inhibits mycelial expansion and attenuates the pathogenicity of *Botrytis cinerea* through the induction of autophagy and apoptosis. Correspondingly, in this study, multiple pathways, such as the cell cycle, MAPK signal pathway were activated in *C. asianum* treated with Fusaricidin extract. These results found from the RNA-seq analysis that Fusaricidin extract could impact the gene transcription involved in cell cycle, MAPK signaling pathway and cell autophagy, resulting in metabolic disorders of *C. asianum* HNI6.

## 5. Conclusion

In conclusion, our study demonstrated that *P. polymyxa* ZJU11 displayed a powerful biocontrol potential in controlling postharvest mango anthracnose. This antagonistic activity is primarily attributed to Fusaricidin-type compounds produced by *P. polymyxa* ZJU11. Using GC-MS/MS analysis, four Fusaricidin variants (A, B, C, and D) were identified. Further mechanistic studies revealed that the antifungal action of Fusaricidin targets the cell membrane of *Colletotrichum* species, resulting in loss of membrane integrity and subsequent cell death. Additionally, transcriptomic and physiological analyses suggest that Fusaricidin may affect critical cellular processes in *C. asianum* HNI6, including the cell cycle, MAPK signaling pathway, and cell autophagy. Therefore, these results support the potential application of *P. polymyxa* ZJU11 as a promising biocontrol strategy for managing postharvest anthracnose in mangoes.

## CRediT authorship contribution statement

**Jinping Cao:** Validation, Methodology, Investigation. **Chongde Sun:** Writing – review & editing, Supervision, Funding acquisition. **Yue Wang:** Writing – review & editing. **Chaoyi Hu:** Software, Methodology. **Cui Sun:** Writing – review & editing, Writing – original draft, Software, Resources, Methodology. **Yihan Wang:** Software, Methodology. **Yihu**

**Pi:** Visualization, Software.

## Declaration of Competing Interest

The authors declare that they have no known competing financial interests or personal relationships that could have appeared to influence the work reported in this paper.

## Acknowledgments

This study was financially supported by Hainan Province Science and Technology Special Fund (grant number: ZDYZ2025XDNY092) and Hainan Provincial Natural Science Foundation of China (grant number: 325RC802).

## Appendix A. Supporting information

Supplementary data associated with this article can be found in the online version at [doi:10.1016/j.postharvbio.2025.114148](https://doi.org/10.1016/j.postharvbio.2025.114148).

## Data availability

Data will be made available on request.

## References

- Aguirre-Guitron, L., Calderon-Santoyo, M., Bautista-Rosales, P.U., Ragazzo-Sanchez, J.A., 2019. Application of powder formulation of *Meyerozyma caribbea* for postharvest control of *Colletotrichum gloeosporioides* in mango (*Mangifera indica* L.). *LWTFood Sci. Technol.* 113, 108271. <https://doi.org/10.1016/j.lwt.2019.108271>.
- Chikez, H., Maier, D., Sonka, S., 2021. Mango postharvest technologies: an observational study of the yieldwise initiative in Kenya. *Agriculture* 11 (7), 623. <https://doi.org/10.3390/agriculture11070623>.
- Chutima, K., Tida, D., 2023. Biocontrol ability of marine yeasts against postharvest diseases in mangoes caused by *Colletotrichum gloeosporioides* and *Lasiopodiplodia theobromae*. *Eur. J. Plant Pathol.* 168 (4), 709–721. <https://doi.org/10.1007/s10658-023-02795-9>.
- Faisal, S., Moshe, D., Steven, A.S., Jeffrey, K.B., 2025. Development and feasibility of an approach utilizing modified atmosphere packaging (MAP) and ethylene scrubbing to allow extended international transport and marketing of tree-ripe mangoes. *Postharvest Biol. Technol.* 225, 113488. <https://doi.org/10.1016/j.postharvbio.2025.113488>.
- Gong, W., Sun, Y., Tu, T., Huang, J., Zhu, C., Zhang, J., Salah, M., Zhao, L., Xia, X., Wang, Y., 2024. Chitosan inhibits *Penicillium expansum* possibly by binding to DNA and triggering apoptosis. *Int. J. Biol. Macromol.* 259 (Part 1), 129113. <https://doi.org/10.1016/j.ijbiomac.2023.129113>.
- Guirado-Manzano, L., Tienda, S., Gutiérrez-Barranquero, J.A., de Vicente, A., Cazorla, F.M., Arrebola, E., 2024. Biological control and cross infections of the *Neofusicoccum* spp. causing mango postharvest rots in Spain. *Horticulturae* 10 (2), 166. <https://doi.org/10.3390/horticulturae10020166>.
- Huang, J., Chen, S.Y., He, W.P., Xiao, Y.N., Wang, N.N., Huang, L.L., 2025. Phenazine-1-carboxylic acid has a broad-spectrum antifungal effect by targeting isocitrate lyase. *J. Agric. Food Chem.* 73 (9), 5007–5019. <https://doi.org/10.1021/acs.jafc.4c08303>.
- Ji, J.Y., Yang, J., Zhang, B.W., Wang, S.R., Zhang, G.C., Lin, L.N., 2020. Sodium pheophorbide a controls cherry tomato gray mold (*Botrytis cinerea*) by destroying fungal cell structure and enhancing disease resistance-related enzyme activities in fruit. *Pest. Biochem. Physiol.* 166, 104581. <https://doi.org/10.1016/j.pestbp.2020.104581>.
- Ko, S.R., Lee, Y.K., Srivastava, A., Park, S.H., Ahn, C.Y., Oh, H.M., 2019. The selective inhibitory activity of a Fusaricidin derivative on a bloom-forming cyanobacterium, *microcystis* sp. *J. Microbiol. Biotechnol.* 29 (1), 59–65. <https://doi.org/10.4014/jmb.1804.04031>.
- Konsue, W., Dethoup, T., Limtong, S., 2020. Biological control of fruit rot and anthracnose of postharvest mango by antagonistic yeasts from economic crops leaves. *Microorganisms* 8 (3), 317. <https://doi.org/10.3390/microorganisms8030317>.
- Lee, B.Y., Chen, P.L., Chen, C.Y., 2024. Suppression of strawberry anthracnose by *Paenibacillus polymyxa* TP3 in situ and from a distance. *Plant Dis.* 108 (3), 700–710. <https://doi.org/10.1094/PDIS-08-23-1499-RE>.
- Li, Y.L., Chen, S.S., 2019. Fusaricidin produced by *Paenibacillus polymyxa* WLY78 induces systemic resistance against Fusarium wilt of cucumber. *Int. J. Mol. Sci.* 20 (20), 5240. <https://doi.org/10.3390/ijms20205240>.
- Li, J., Jensen, S.E., 2008. Nonribosomal biosynthesis of fusaricidins by *Paenibacillus polymyxa* PKB1 involves direct activation of a D-amino acid. *Chem. Biol.* 15 (2), 118–127. <https://doi.org/10.1016/j.chembiol.2007.12.014>.
- Lin, S.Y., Chen, X.H., Xie, L., Zhang, Y., Zeng, F.H., Long, Y.Y., Ren, L.Y., Qi, X.L., Wei, J.G., 2023a. Biocontrol potential of lipopeptides produced by *Paenibacillus polymyxa* AF01 against *Neoscytalidium dimidiatum* in pitaya. *Front. Microbiol.* 14, 1188722. <https://doi.org/10.3389/fmicb.2023.1188722>.
- Lin, W.L., Duan, C.H., Wang, C.L., 2023b. Identification and virulence of *Colletotrichum* species causing anthracnose on mango. *Plant Pathol.* 72 (3), 623–635. <https://doi.org/10.1111/ppa.13682>.
- Ma, D.Y., Cui, X.M., Zhang, Z.Q., Li, B.Q., Xu, Y., Tian, S.P., Chen, T., 2020. Honokiol suppresses mycelial growth and reduces virulence of *Botrytis cinerea* by inducing autophabic activities and apoptosis. *Food Microbiol.* 88, 103411. <https://doi.org/10.1016/j.fm.2019.103411>.
- Montiel, L.G.H., Rodriguez, R.Z., Angulo, C., Puente, E.O.R., Aguilar, E.E.Q., Galicia, R., 2017. Marine yeasts and bacteria as biological control agents against anthracnose on mango. *J. Phytopathol.* 165 (11–12), 833–840. <https://doi.org/10.1111/jph.12623>.
- Muelner, P., Schwarz, E., Dietel, K., Herfort, S., Jaehne, J., Lasch, P., Cernava, T., Berg, G., Vater, J., 2021. Fusaricidins, polymyxins and volatiles produced by *Paenibacillus polymyxa* strains DSM 32871 and M1. *Pathogens* 10 (11), 1485. <https://doi.org/10.3390/pathogens10111485>.
- Qian, L., Ying, Z., Xiaoman, Z., Yanli, X., 2021. Antifungal efficacy of paeonol on *Aspergillus flavus* and its mode of action on cell walls and cell membranes. *LWTFood Sci. Technol.* 149, 111985. <https://doi.org/10.1016/j.lwt.2021.111985>.
- Ren, W.C., Liu, N., Sang, C.W., Shi, D.Y., Zhou, M.G., Chen, C.J., Qin, Q.M., Chen, W.C., 2018. The autophagy gene BcATG8 regulates the vegetative differentiation and pathogenicity of *Botrytis cinerea*. *Appl. Environ. Microbiol.* 84 (11), e02455–02417. <https://doi.org/10.1128/AEM.02455-17>.
- Sant, D.G., Tupe, S.G., Ramana, C.V., Deshpande, M.V., 2016. Fungal cell membrane-promising drug target for antifungal therapy. *J. Appl. Microbiol.* 121 (6), 1498–1510. <https://doi.org/10.1111/jam.13301>.
- Vater, J., Niu, B., Dietel, K., Borriss, R., 2015. Characterization of novel fusaricidins produced by *Paenibacillus polymyxa*-M1 using MALDI-TOF mass spectrometry. *J. Am. Soc. Mass Spectrom.* 26 (9), 1548–1558. <https://doi.org/10.1007/s13361-015-1130-1>.
- Vecchio, L., Vitale, A., Aiello, D., Di Pietro, C., Parafati, L., Polizzi, G., 2025. Prevalence of *Neofusicoccum parvum* associated with fruit rot of mango in south Italy and its biological control under postharvest conditions. *J. Fungi* 11 (5), 384. <https://doi.org/10.3390/jof11050384>.
- Wang, Y., Liu, X.Y., Chen, T., Xu, Y., Tian, S.P., 2020. Antifungal effects of hinokitiol on development of *Botrytis cinerea* in vitro and in vivo. *Postharvest Biol. Technol.* 159, 111038. <https://doi.org/10.1016/j.postharvbio.2019.111038>.
- Wu, Y., Cheng, J.H., Sun, D.W., 2022. Subcellular damages of *Colletotrichum asiaticum* and inhibition of mango anthracnose by dielectric barrier discharge plasma. *Food Chem.* 381, 132197. <https://doi.org/10.1016/j.foodchem.2022.132197>.
- Wu, F., Tong, X.Q., Zhang, L.Q., Mei, L., Guo, Y.B., Wang, Y.J., 2020. Suppression of *Rhizophus* fruit rot by volatile organic compounds produced by *Paenibacillus polymyxa* CF05. *Biocontrol Sci. Technol.* 30 (12), 1351–1364. <https://doi.org/10.1080/09583157.2020.1826902>.
- Xie, Q., Huang, L., Xiao, Q., Luo, H., Wang, Q., An, B., 2025. Berberine synergistically enhances iprodione's antifungal activity against *Colletotrichum gloeosporioides*. *Postharvest Biol. Technol.* 223, 113454. <https://doi.org/10.1016/j.postharvbio.2025.113454>.
- Yang, Y., Dong, G.R., Wang, M., Xian, X.W., Wang, J., Liang, X.Y., 2021. Multifungicide resistance profiles and biocontrol in *Lasiopodiplodia theobromae* from mango fields. *Crop Prot.* 145, 105611. <https://doi.org/10.1016/j.cropro.2021.105611>.
- Yang, F., Jiang, H.Y., Ma, K., Hegazy, A., Wang, X., Liang, S., Chang, G.Z., Yu, L.Q., Tian, B.M., Shi, X.J., 2024. Genomic and phenotypic analyses reveal *Paenibacillus polymyxa* PJH16 is a potential biocontrol agent against cucumber fusarium wilt. *Front. Microbiol.* 15, 1359263. <https://doi.org/10.3389/fmicb.2024.1359263>.
- Yang, A.M., Zeng, S., Yu, L., He, M., Yang, Y.Y., Zhao, X.Z., Jiang, C.L., Hu, D.Y., Song, B.A., 2018. Characterization and antifungal activity against *Pestalotiopsis* of a fusaricidin-type compound produced by *Paenibacillus polymyxa* Y-1. *Pest. Biochem. Physiol.* 147, 67–74. <https://doi.org/10.1016/j.pestbp.2017.08.012>.
- Zeng, R., Zou, X.X., Huang, C., Si, H.Y., Song, J., Zhang, J., Luo, H., Wang, Z.D., Wang, P., Fan, G.R., Rao, X.P., Liao, S.L., Chen, S.X., 2023. Novel design of citral-thiourea derivatives for enhancing antifungal potential against *Colletotrichum gloeosporioides*. *J. Agric. Food Chem.* 71 (7), 3173–3183. <https://doi.org/10.1021/acs.jafc.2c07851>.
- Zhang, S.P., Guo, Y., Li, S.Z., Li, H., 2022. Histone acetyltransferase CfGcn5-mediated autophagy governs the pathogenicity of *Colletotrichum fructicola*. *Mbio* 13 (5). <https://doi.org/10.1128/mbio.01956-22>.
- Zhang, Q.X., Xing, C.L., Li, S.Y., He, L.L., Qu, T.L., Chen, X.J., 2021. In vitro antagonism and biocontrol effects of *Paenibacillus polymyxa* JY1-5 against *Botrytis cinerea* in tomato. *Biol. Control* 160, 104689. <https://doi.org/10.1016/j.biocontrol.2021.104689>.
- Zhou, D., Jing, T., Chen, Y., Yun, T., Yun, Qi, D., Zang, X., Zhang, M., Wei, Y., Li, K., Zhao, Y., Wang, W., Xie, J., 2022. Biocontrol potential of a newly isolated *Streptomyces* sp. HSL-9B from mangrove forest on postharvest anthracnose of mango fruit caused by *Colletotrichum gloeosporioides*. *Food Control* 135, 108836. <https://doi.org/10.1016/j.foodcont.2022.108836>.
- Zou, X., Wei, Y., Jiang, S., Xu, F., Hongfei, W., Zhan, P., Shao, X., 2022. ROS stress and cell membrane disruption are the main antifungal mechanisms of 2-phenylethanol against *Botrytis cinerea*. *J. Agric. Food Chem.* 70 (45), 14468–14479. <https://doi.org/10.1021/acs.jafc.2c06187>.
- Zuo, C.W., Zhang, W.N., Chen, Z.J., Chen, B.H., Huang, Y.H., 2017. RNA sequencing reveals that endoplasmic reticulum stress and disruption of membrane integrity underlie dimethyl trisulfide toxicity against *Fusarium oxysporum* f. sp. *cubense* tropical race 4. *Front. Microbiol.* 8, 1365. <https://doi.org/10.3389/fmicb.2017.01365>.